INFLUENCE OF BRAIDED SLEEVES ON THE IMPACT DAMAGE OF CYLINDRICAL UNIDIRECTIONAL ELEMENTS

D. N. Allen[1], D. W. Jensen[1]*, M. D. Embley[1], M. J. Jensen[2]
[1] Civil and Environmental Engineering, Brigham Young University, Provo UT, USA,
[2] Altus Poles, Inc., Provo, UT, USA
* Corresponding author (david@byu.edu)

Keywords: damage tolerance, unidirectional, braided sleeves, compression strength after impact

1 Introduction

The influence of co-cured encapsulating sleeves on the damage tolerance (specifically, the compression strength after impact) of solid cylindrical elements composed of unidirectional basalt/epoxy composite materials has been quantified. These structural elements represent local members of three-dimensional open lattice (grid) structures (e.g., based on IsoTruss® or isogrid technology, etc.) that are continuously fabricated using advanced three-dimensional braiding techniques [1]. Small, solid, cylindrical samples, nominally about 8 mm (5/16 in) in diameter, composed of unidirectional basalt fibers were fabricated with various aramid sleeve configurations (i.e., with varied coverage and sleeve patterns). The surface coverage of the sleeves ranged from approximately half to full coverage. Both bi-directional braids and uni-directional spiral wraps were investigated. Five specimens of each configuration were impacted with a cylindrical steel impactor at energy levels of approximately 5 J (3.7 ft-lbs) and 10 J (7.4 ft-lbs), and tested to determine residual compression strength after impact.

2 Background

Because advanced composite materials are typically brittle, and members of grid structures are composed of unidirectional fibers, even small impact energies could potentially significantly degrade mechanical properties. Damage in composites is generally difficult to detect since the local damage caused by the impact is usually internal, or on the opposite side of the impact. Open lattice structures have the advantage with respect to damage monitoring, since all sides of each member are visible, but what's happening inside the composite members is still unknown.

Braided sleeves have previously been shown to improve damage tolerance behavior of unidirectional elements by absorbing and dispersing some of the impact energy and by containing internal damage. In a secondary operation, Winsom [2] added braided aramid sleeves to fully-cured carbon fiber pultruded rods, increasing the compression strength after impact by approximately 50%. The braided sleeves created a transverse compressive stress that confined the core fibers and increased the effective tensile strength of the matrix in the transverse direction [3]. In the current research, the external sleeves were used for consolidation (Fig. 1) and, therefore, co-cured with the unidirectional fibers in the core.

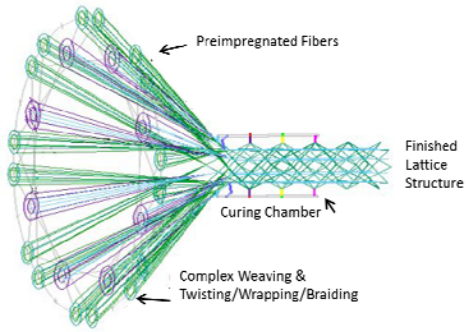

Fig. 1. Sketch of automated continuous composite lattice fiber paths.

3 Experimental Procedures

3.1 Materials

This research utilized unidirectional basalt fibers wrapped in aramid sleeves. The basalt was Kameny Vek's continuous fiber roving 13.1200 KV12, with a

filament diameter of 13 µm ($5.1x10^{-7}$ in), fiber tensile strength of 2.8-3.0 GPa (406-435 ksi), and fiber tensile modulus of 87-90 GPa (12,300-13,000 ksi). The basalt fibers were pre-impregnated by TCR Composites with UF3330-100 resin, designed for low heat applications and long-term room-temperature storage. The sleeves were composed of Kevlar 49, 7100 denier, dry fiber, selected for its winding characteristics.

3.2 Specimen Geometry

The specimens tested were nominally 7.9 mm (5/16") in diameter, yielding an average cross-sectional area of 52 mm^2 (0.085 $inch^2$), with a standard deviation for each configuration less than 2%. Designed for strength-controlled failure, the specimens were 114 mm (4.5") overall, with an unsupported length of 76 mm (3"). Preliminary testing showed that only specimens that were not impacted failed in the manner expected for compression, forming a kink band [4]. Although difficult to substantiate, the impacted specimens appeared to be susceptible to buckling, with an effective hinge at the impact damage locations.

3.3 Specimen Preparation

The specimens were fixed in steel end caps with epoxy (Fig. 2), a test-ready specimen showing the prepared end surface. A completely flat surface normal to the loading axis ensured proper load introduction. An alignment fixture was used to ensure that the specimen was parallel to the loading axis to diminish p-delta effects [5].

Fig. 2. Test-ready specimen: elevation view (left); and, end view (right).

3.4 Impact Energies

Damage was inflicted using a Dynatup® 8200 drop weight impact test machine with a cylindrical tup, to prevent glancing blows. Specimens impacted with nominal total energies of 5-10 J (3.7-7.4 ft-lbs) were compared to undamaged control specimens. The energy levels were based on their approximate 1/3 and 2/3 reduction in compressive strength after impact, respectively, compared to undamaged specimens. Total impact energy is not a direct measure of actual damage inflicted on the composite materials, but provides a consistent basis for comparison. Absorbed energy would more closely relate to actual damage levels [6].

3.5 Testing

Compressive strength after impact tests were conducted in a specially-fabricated test setup. The prepared test specimens were inserted into the steel specimen receptacles, which were, in turn, clamped into an 89 kN (20 kip) Instron compression machine. The specimen receptacles were designed with side walls to align the specimens and facilitate testing. Tungsten-carbide pucks were inserted between the horizontal interfaces of the specimen and receptacles, to prevent the creation of surface defects in the receptacle by the specimens (Fig. 3). The specimens were loaded at a rate of 0.127 cm/min (0.05 in/min), while recording axial compressive load, machine displacement, and displacement from a 25-mm (1.0-in) extensometer for local strain.

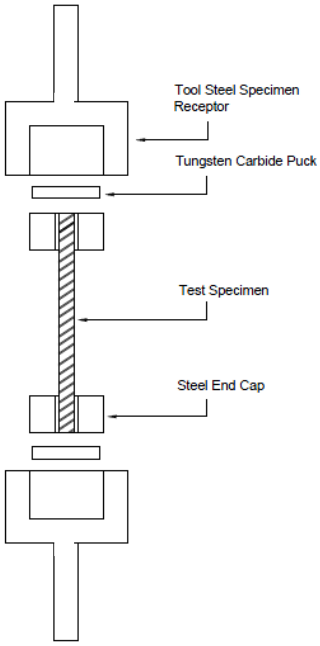

Fig. 3. Expanded view of test specimen and fixture.

4 Compression Test Results

For each test configuration, a compressive stress vs. strain plot (example shown in Fig. 4) was created showing each individual specimen and an average curve for the entire group.

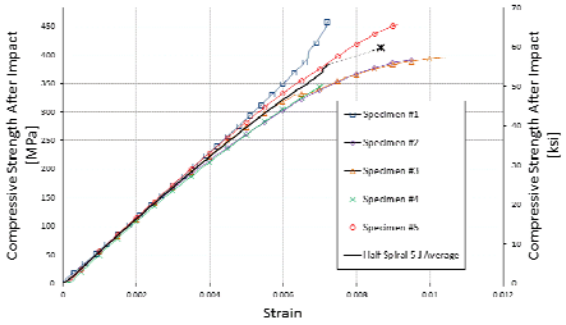

Fig. 4. Compression stress-strain curves for spiral-wrapped specimens with half sleeve coverage impacted at 5 J (3.7 ft-lbs).

A summary of the average ultimate compression stress for each configuration is shown in Table 1. Summaries of the average maximum compression strain and average compression modulus of elasticity for each configuration are shown in Tables 2 and 3, respectively.

Table 1. Average ultimate compression strengths.

Specimen Configuration & Impact Energy		Ultimate Compression Stress		
		Avg. Max. [MPa (ksi)]	Std. Dev. [MPa (ksi)]	[%]
Full Braid	0 J	722 (105)	13.9 (2.02)	1.9
	5 J	490 (71.0)	65.7 (9.53)	13
	10 J	301 (43.6)	22.4 (3.26)	7.5
Half Braid	0 J	743 (108)	87.4 (12.7)	12
	5 J	546 (79.3)	86.7 (12.6)	16
	10 J	233 (33.7)	53.1 (7.70)	22
Full Spiral	0 J	732 (106)	83.4 (12.1)	11
	5 J	530 (76.8)	7.08 (1.03)	1.3
	10 J	334 (48.5)	19.0 (2.75)	5.7
Half Spiral	0 J	647 (93.9)	97.4 (14.1)	15
	5 J	412 (59.7)	47.6 (6.91)	12
	10 J	232 (33.7)	36.8 (5.33)	16

Table 2. Average maximum compression strains.

Specimen Configuration & Impact Energy		Maximum Compression Strain		
		Average Max [10^3 με]	Std. Dev. [10^3 με]	[%]
Full Braid	0 J	13.8	7.00	51
	5 J	8.73	1.69	19
	10 J	11.8	5.50	47
Half Braid	0 J	12.7	3.66	29
	5 J	11.2	3.17	28
	10 J	10.5	7.95	76
Full Spiral	0 J	14.2	6.20	44
	5 J	8.66	2.17	25
	10 J	12.1	6.60	55
Half Spiral	0 J	10.7	1.83	17
	5 J	8.68	1.47	17
	10 J	8.03	1.12	14

Table 3. Average compression modulus of elasticity.

Specimen Configuration & Impact Energy		Compression Young's Modulus		
		Average Max [GPa (10^6 psi)]	Std. Dev. [GPa (10^6 psi)]	[%]
Full Braid	0 J	69.5 (10.1)	11.3 (1.64)	16
	5 J	61.8 (8.97)	8.89 (1.29)	14
	10 J	50.0 (7.26)	0.74 (0.11)	1
Half Braid	0 J	64.4 (9.34)	7.27 (1.05)	11
	5 J	61.4 (8.90)	5.29 (0.77)	8.6
	10 J	53.3 (7.73)	32.3 (4.69)	61
Full Spiral	0 J	61.3 (8.89)	6.30 (0.91)	10
	5 J	64.8 (9.39)	4.44 (0.64)	6.9
	10 J	55.1 (7.99)	11.1 (1.61)	20
Half Spiral	0 J	60.3 (8.75)	4.05 (0.59)	6.7
	5 J	55.6 (8.06)	1.95 (0.28)	3.5
	10 J	47.9 (6.95)	8.23 (1.19)	17

5 Discussions of Results

5. 1 Plot of Compression Stress vs. Strain

In Table 4, the average compression stress-strain response as a function of the coverage and sleeve configuration is compared for each level of damage. When comparing coverage, the quantities in the table include values from both braid and spiral sleeve specimens. Likewise, when comparing the sleeve type, the table includes the results from both full and half coverage.

With no damage inflicted on the specimen, there is only a 5% decrease in compression strength as a consequence of decreasing from full to half coverage. There is also a 5% reduction in compression strength with the spiral wrap compared to the braided sleeve.

At an impact energy of 5 J (3.7 ft-lbs), the decrease in compression strength is similar to specimens that were not impacted, with only a slight decrease in strength going from both full coverage and braided sleeve to half coverage and spiral wrap, respectively.

At a nominal impact energy of 10 J (7.4 ft-lbs), a substantial decrease, 29%, in compression strength occurs from full to half coverage (also visible in Fig. 6 for braid coverage and Fig. 7 for type of sleeve).

Table 4. Effect of sleeve configuration on compression strength.

Configuration Comparison	Compression Strength [MPa (ksi)]		
	No Impact	5-J Impact (3.7 ft-lbs)	10-J Impact (7.4 ft-lbs)
Influence of Sleeve Surface Coverage			
Full Coverage	727 (105)	510 (73.9)	317 (46.0)
Half Coverage	690 (100)	479 (69.5)	232 (33.7)
Difference	-5%	-6%	-27%
Influence of Sleeve Type			
Braided Sleeve	733 (106)	519 (75.2)	266 (38.6)
Spiral Sleeve	696 (101)	471 (68.3)	283 (41.1)
Difference	-5%	-9%	6%

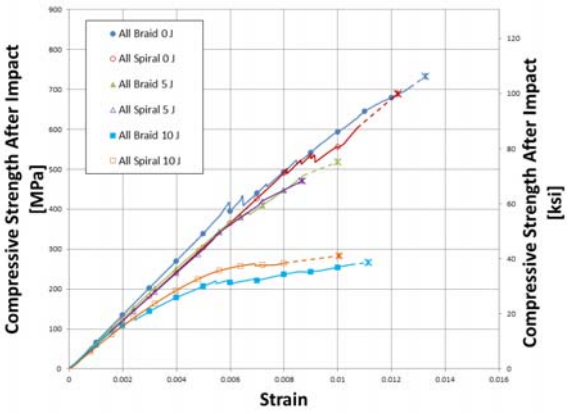

Fig. 6. Average compression stress-strain curves for braid and spiral sleeves.

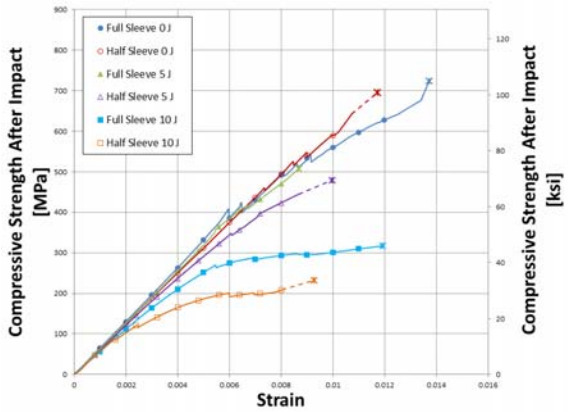

Fig. 7. Average compression stress-strain curves of full and half coverage.

The average compression stress-strain curves for all sleeve configurations and impact energies are plotted in Fig. 8. The curves are bounded on the upper end by the undamaged specimens, with all damaged specimens falling under this envelope, as expected. Non-impacted specimens and those impacted at 5 J (3.7 ft-lbs) are closely grouped, irrespective of sleeve configuration. Specimens impacted with 10 J (7.4 ft-lbs) exhibit more scatter, consistent with the results in Table 4. The curves in Fig. 8 also reveal the difficulties using an extensometer to measure displacements on a braided surface. The jogs in the curves occur when the blades of the extensometer apparently slip down the aramid ridges, or perhaps the tow loosens under compression load.

5.2 Plot of Compression Stress vs. Impact Energy

A plot of the compression strength as a function of impact energy is shown in Figure 9. Each specimen is represented in this plot, and a dashed curve is fitted to the average values at impact energy, to show the trend for each sleeve configuration. All configurations are nearly equal when there has been no impact damage. Subjected to only relatively light impact, 5 J (3.7 ft-lbs), the configuration with only half coverage performed better than a full braid. This is counter-intuitive, and not yet completely understood. Subjected to more severe damage, 10 J (7.4 ft-lbs), the configuration with a full spiral wrap maintains its strength best after impact. Again this is counter-intuitive and underscores the need for further research.

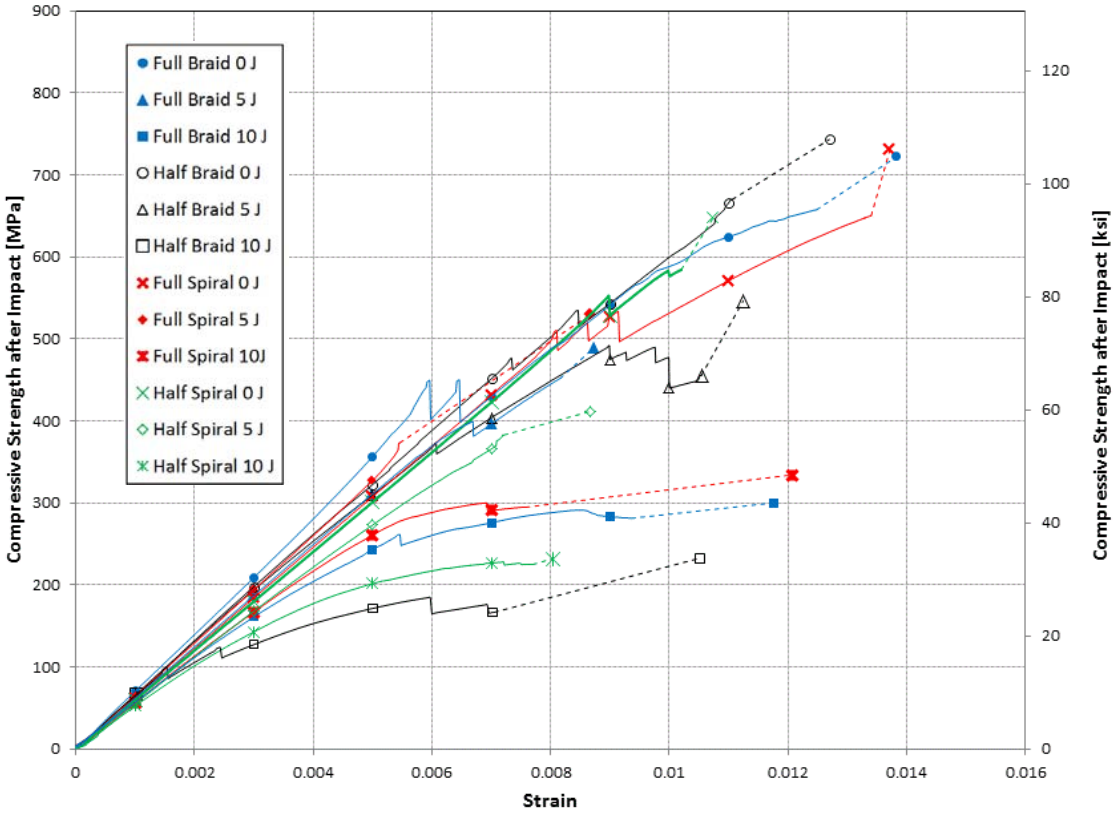

Fig. 8. Average compression stress-strain curves for all sleeve configurations and impact energies.

6 Conclusions

The compression behavior of unidirectional basalt/epoxy composite rods subjected to light and severe impact has been quantified. The type of sleeve (braid vs. spiral) and the amount of coverage (full vs. half) affect the compression behavior. With no impact, there is virtually no difference in compression behavior for the different sleeve configurations used to consolidate the cores during manufacturing. This also holds true for light impact damage, 5 J (3.7 ft-lbs). With more severe impact damage, 10 J (7.4 ft-lbs), however, half coverage of the unidirectional fibers results in a substantial decrease in strength (26%) relative to specimens having full sleeve coverage. This preliminary research demonstrates that braided sleeves can be used to successfully consolidate bundles of unidirectional fibers, and simultaneously provide significant improvement in damage tolerance.

7 Acknowledgements

The authors would like to gratefully acknowledge the support of Novatek, Inc., the sponsor of this research, under the leadership of Mr. David Hall, and all of the Novatek, Altus Poles, and Brigham Young University employees who helped enable this research, especially Mr. Craig Garvin, of Novatek, Inc., and Mr. Alex DeBirk, an undergraduate research assistant at Brigham Young University.

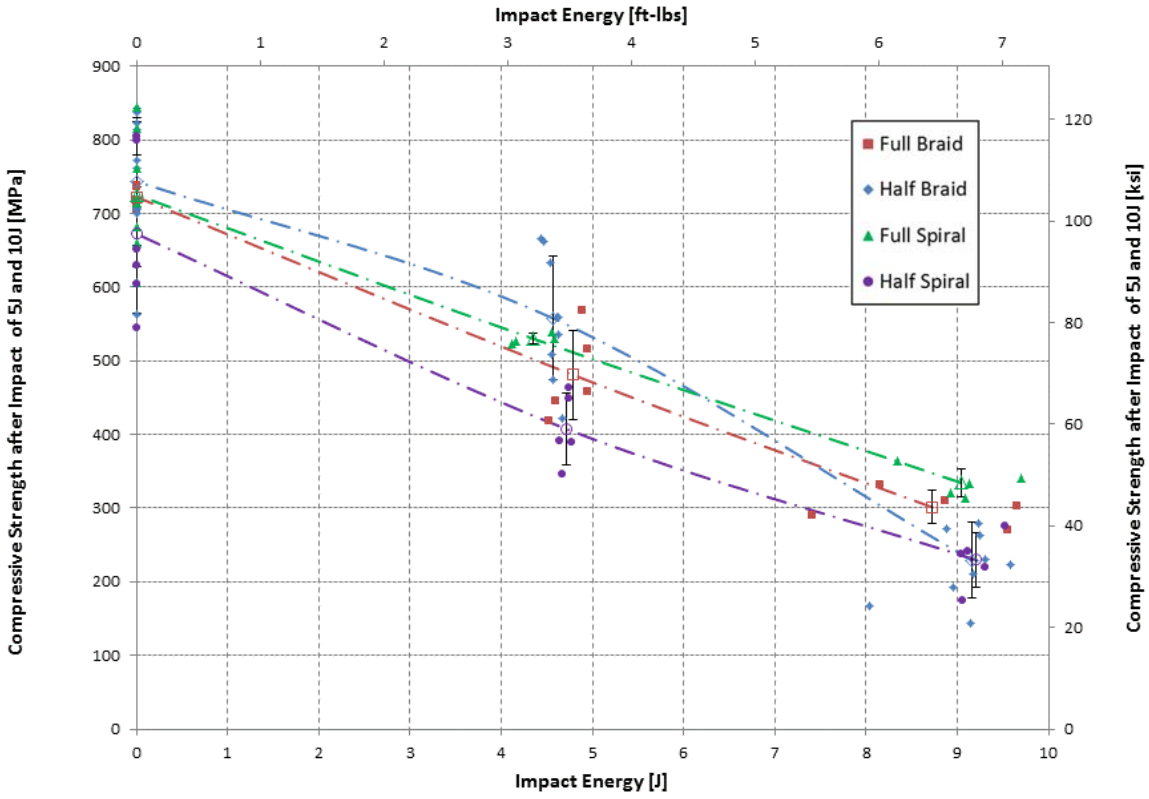

Fig. 9. Compression strength after impact for all sleeve configurations.

8 References

[1] S. Kesler "Consolidation and Interweaving of Composite Members by a Continuous manufacturing Process," M.S. Thesis, Brigham Young University, Provo, Utah, December 2006.

[2] M. Wisnom "Suppression of splitting and impact sensitivity of unidirectional carbon-fibre composite rods using tensioned overwind." *Composites Part A: Applied Science and Manufacturing*, Vol. 30, No. 5, pp. 661-5, 1999.

[3] S. Hansen "Influence of Consolidation and Interweaving on Compression Behavior of IsoTruss® Structures," M.S. Thesis, Brigham Young University, Provo, Utah, April 2004.

[4] Schuap, J. Mahy, M. Andrews, O. Grabandt, R. Young "Compressive behavior of aramid fiber-reinforced pultruded rods." *Journal of Composite Materials*, Vol. 32, No. 9, pp. 893-908, 1998.

[5] C. Stoutis "Compression testing of pultruded carbon fibre-epoxy cylindrical rods." *Journal of Materials Science*, Vol. 34, pp. 3441-3446, 2000.

[6] J. Hartness, P. Sjoblom, T. Cordell "On low-velocity impact testing of composite materials." *Journal of Composite Materials*, Vol. 22, No. 1, pp. 30-52, 1988.